Hydro-Mechanical Modelling of Multiphase Flow in Coalbed by Computational Homogenization

François Bertrand[1,2,3(✉)], Olivier Buzzi[2], and Frédéric Collin[1]

[1] University of Liège, Liège, Belgium
francois.bertrand@uliege.be
[2] University of Newcastle, Callaghan, Australia
[3] F.R.I.A FNRS, Liège, Belgium

Abstract. A multiscale model is developed for the modelling of coalbed methane (CBM) production. CBM recovery is known to be a highly coupled and multiphase problem. The finite element square method is used to integrate a fracture-scale model in a multiscale scheme. This method consists to localize the macroscale deformation to the microscale, then resolve the boundary value problem on the microscale with finite elements, then homogenize the microscale stresses to compute macroscopic quantities, and finally resolve the boundary value problem on the macroscale with finite elements. This approach has the advantage that it does not require to write some constitutive laws at the macroscale but only at the REV-scale. The multiscale model is therefore appropriate for reservoir modelling. The model is developed and implemented in a finite element code and the simulation of a synthetic reservoir is considered.

Keywords: Numerical model · FE^2 · Permeability · Fractured medium · Couplings · Langmuir · Shrinkage

1 Introduction

In existing CBM models, sorption- and stress-induced coal permeability alteration is a remarkable aspect which is often improperly simplified. Ideally, a numerical model would detail the material microstructure with separate descriptions of each constituent. Given the high computational expense it would require, this approach is not possible at the reservoir scale. A microscale model has therefore to be integrated in a multiscale scheme.

In this work, the finite element method is used for both the microscale and the macroscale, it is the finite element square method (FE^2). This method was first applied to deal with heat conduction problems Özdemir et al. (2008). Then, it was used for the modelling of saturated porous media (Su et al. 2011; Marinelli 2013; Van den Eijnden 2015). In the context of CBM recovery, the method has to be extended to partially saturated media. To our knowledge, the FE^2 method has never been applied to coal before.

M. Barla et al. (Eds.): IACMAG 2021, LNCE 125, pp. 600–607, 2021.
https://doi.org/10.1007/978-3-030-64514-4_61

In the following, the hydro-mechanical multiscale model is first presented. Then, it is applied for reservoir modelling with a synthetic case to demonstrate the ability of the model to obtain the expected production curves for CBM recovery.

2 Hydro-Mechanical Model

2.1 Decomposition of the Microkinematics

The micromechanical displacement field u_i^m is decomposed in the macromechanical field u_i^M and a fluctuation displacement field u_i^f:

$$u_i^m(p) = u_i^M(\hat{p}) + \frac{\partial u_i^M(\hat{p})}{\partial xj}(x_j - \hat{x}_j) + u_i^f(\hat{p}) \tag{1}$$

This fluctuation field results of the variations in material properties within the REV. It represents therefore the fine scale deviations with respect to the average fields. Water pressure p_w and gas pressure p_g are also introduced to develop the multiphase model. As for the microscale displacements, the fluid microscale pressure fields can be decomposed into macroscale components and microkinematical fluctuations.

2.2 Periodic Boundary Conditions

The macroscopic deformation enters the microscale BVP through the boundary conditions. The periodic boundary conditions are adopted for their efficiency to transfer the macroscale deformation to the microscale REV (Van der Sluis et al. 2000). The periodic boundary enclosing the REV is subdivided in two parts: the lead part Γ^L and the follow part Γ^F. The kinematics of any point x^F on the follow boundary Γ^F depends on the kinematics of its homologous x^L on the lead boundary Γ^L. For small strains, the mechanical part of the periodic boundary conditions for the REV is defined in terms of displacements through the relation.

$$u_i^F = u_i^L + \varepsilon_{ij}^M(x_j^F - x_j^L) \tag{2}$$

Where ε_{ij}^M is the macroscopic Cauchy strain. In the same way, the boundary conditions for water and gas pressures, p_w and p_g, are given by

$$p_{w/g}^F = p_{w/g}^L + \nabla p_{w/g}^M(x_j^F - x_j^L) \tag{3}$$

Moreover, the periodic boundary conditions lead to the requirement of the antisymmetry of the boundary traction and boundary fluxes.

2.3 Separation of Scales

The statement $u_i^m(\hat{P}) = u_i^M(\hat{P})$ has to hold in Eq. (1) for any point of the macroscale. It follows that

$$\frac{\partial u_i^M(\hat{p})}{\partial x_j}(x_j - \hat{x}_j) + u_i^f(\hat{p}) \ll u_i^M(\hat{p}) \tag{4}$$

The validity of the approach is therefore theoretically restricted to situations where the scale of variation of the macroscopic fields is large compared to the microstructure and its REV. The microscopic characteristic length is reasonably the REV size l_{REV}. The macroscopic length depends on the macroscopic gradient of fluid pressure ∇p^M and the macroscopic pressure p^M. We have therefore to verify that

$$l_{REV} \ll \frac{p^M}{\nabla p^M} \tag{5}$$

to satisfy the separation of scales.

Moreover, as the size of the REV/unit cell should be very small compared to the macroscale, it is generally consistent to assume the hydraulic flow at the micro level is insensitive to the time variations of the fluid storage at this level. In other words, the microscale problem may be solved under steady-state conditions.

2.4 Microscale Balance Equations

Neglecting the body forces, the equilibrium of the REV means the Cauchy stress tensor has to satisfy:

$$\frac{\partial \sigma_{ij}^m}{\partial x_j} = 0 \tag{6}$$

In addition to the mechanical equilibrium, the mass balance equations for water and gas are

$$M^m/_{w/g} + \frac{\partial f_{w/g_i}^m}{\partial x_i} = 0 \tag{7}$$

where f_{w/g_i}^m are the internal total fluxes of water or gas. Under the assumption of steady state at the microscale, the variations of the fluid contents vanish out.

2.5 Microscale Constitutive Laws

The constitutive microscale model is constituted of some mechanical laws for the matrix and the fracture. The microscale model shortly described hereafter is based on developments presented by (Bertrand et al. 2019).

2.5.1 Matrix

Solid constitutive law: The elastic law considering sorption-induced strain writes

$$\Delta\sigma_{ij} = 2G_m\Delta\varepsilon_{ij} + \lambda_m\Delta\bar{\varepsilon}\delta_{ij} + K_m\Delta\varepsilon_{v_s}\delta_{ij} \tag{8}$$

where ε_{ij} is the small-strain tensor, $\bar{\varepsilon} = \varepsilon_{ij}\,\delta_{ij}$ with δ_{ij} the Kronecker's symbol, G_m is the Coulomb's modulus and λ_m is the first Lamé parameter, K_m is the bulk modulus of the matrix and $\Delta\varepsilon_{v_s}$ is the volumetric sorption-induced strain. This sorption-induced strain depends on the adsorbed gas content $V_g^{Ad}[m^3/kg]$ and a linear coefficient $\beta_{\in}\left[\mathrm{kg/m^3}\right]$:

$$\Delta\varepsilon_{v_s} = \beta_\varepsilon\Delta V_g^{Ad} \tag{9}$$

Adsorbed gas content evolution: At equilibrium, the adsorbed gas content is given by the Langmuir's isotherm (Langmuir 1918):

$$V_g^{Ad} = \frac{V_L \cdot p}{p_L + p} \tag{10}$$

where $V_L[m^3/kg]$ and $P_L[Pa]$ are the Langmuir's parameters, and $p[Pa]$ depends on the macroscopic fluid pressures (consistent with the separation of scales). If an instantaneous equilibrium is too restrictive, a sorption time can be introduced to take into account the delay imposed by the diffusion process into the matrix (Bertrand et al. 2017).

2.5.2 Cleats

Interface mechanical law: The mechanical law for the interfaces is defined by two parameters, the normal stiffness K_n and tangential stiffness K_s, which define the relation between the stresses and the fracture displacements. The tangential stiffness is considered constant while a Bandis-type law is used for the normal stiffness (hyperbolic evolution with the aperture) (Goodman 1976; Bandis et al. 1983).

Channel flow model: The interface mass flux of water is given by

$$\omega_w = -\rho_w h_b k_{rw}\frac{h_b^2}{12}\frac{1}{\mu_w}\frac{dp_w^m}{ds} \tag{11}$$

Considering the scale separability, the fluid pressure variation is very small compared to the REV size and has a negligible effect on the fluid density. The density is thus considered to be constant throughout the REV. Under isothermal conditions, the water density is only dependent on the macroscale water pressure.

For gas, in addition to the gas advective flow, the interface mass flux also considers dissolved gas in water.

Finally, the relative permeabilities k_{rw} and k_{rg} are only dependent on the macroscale fluid pressures. The relative permeability curves which are used are:

$$k_{rw} = \frac{S_r^2}{2}(3 - S_r) \tag{12}$$

$$k_{rg} = (1 - S_r)^3 \tag{13}$$

where the saturation degree S_r is obtained from the retention curve. A Brooks-Corey model with a distribution index λ is employed (Brooks and Corey 1964).

2.6 Microscale Numerical Solution

The problem is solved iteratively in two parts, starting with the mechanical problem and then finding the different flows for the given fracture apertures. The sequence is repeated until convergence.

2.6.1 Mechanical Part

The weak form of the local momentum balance Eq. (6) governing the microscale BVP is solved numerically using a full Newton-Raphson scheme. The boundary volume is discretized with finite elements. For the matrix, a 4-node element with 4 integration points is adopted for the spatial discretization. For the cleats, one-dimensional elements with 2 integration points are used. The global stiffness matrix establishes the incremental relation between the nodal displacement and the nodal force. This relation is valid for constant fluid pressures.

2.6.2 Hydraulic Part

The explicit description of the fluid network is solved separately from the mechanical problem in order to find the profiles of the gas and water pressures that respect the boundary conditions and, at the same time, have some average values of the pressure fields equal to the macroscopic water and gas pressures. The mass conservation along the channel leads to write that, for each node of the hydraulic network, the sum of the input flows must be equal the sum of output flows.

Moreover, we have to take into account the homologous connectivity of lead and follow node couples over the periodic boundaries and the conditions given by the macroscopic pressure gradient (Eq. 3) to establish the linear system of equations to be solved to find the water pressures. A well-posed system is found by applying the macroscopic pressure at one of the nodes of the hydraulic network. For gas, the mass flux also considers dissolved gas in the water.

2.7 Homogenized Macroscale Response

The micro-to-macro transition is derived from the Hill-Mandel macro-homogeneity condition which requires the average microscale work to be equal to the macroscale work. The macroscopic stress is obtained from the average of the microscopic stresses over the REV.

Concerning the hydraulic part, given the steady state conditions, the macroscale fluxes are the sum of the fluxes on the nodes belonging to the follow boundary. The macroscopic fluid contents are directly defined as the total amounts of fluid in the REV. The fluid mass storage terms are obtained with some finite difference approximations over the time interval Δt.

3 Reservoir Modelling

The multiscale model is applied to the modelling of coalbed methane production from a wellbore. The macroscale mesh and the geometry of the microstructure is given in Fig. 1. The REV is made up few blocks arranged in staggered rows with continuous horizontal cleats. The size of the microstructure is 1 cm over 1 cm. All the parameters defining the reference case are reported in Table 1. The seam is 2 m high and the vertical displacement is blocked on the bottom boundary while a 5 MPa overburden pressure is applied on the top boundary. Axisymmetric conditions are considered around the well on the left side. The smallest element close to the well is 5 cm wide. The size of the elements increases with a geometric factor of 1.5, it means 12 elements represent 13 m. The drained volume is approximately 1000 m^3. An actual reservoir is certainly larger but this synthetic reservoir allows us to test very quickly the capability of the model to reproduce some bell-shape curves since the time to drain the reservoir is not too long.

Water and gas pressures are initialized to 3 MPa, the reservoir is water saturated. Given the overburden pressure of 5 MPa, the effective stress in the cleats is 2 MPa. Note the cleat aperture 20 μm in Table 1 is given for a null stress, as encoded by the user in the Lagamine data file. At the initial effective stress state, the cleat aperture is actually 10 μm and the normal stiffness 225·109 Pa/m. The modelling consists in simulating a drop in the pressure at the well from 3 MPa to 1 MPa in one day. This pressure drawdown causes the water and gas to flow towards the well. The most critical water pressure gradient is observed close to the well at the exact time we stop decreasing the well pressure to maintain it at a constant value of 1 MPa, i.e. at 24 h in this case. At this time, the water pressure profile gives a critical macroscopic characteristic length greater than the REV size anywhere in the mesh.

Water and gas production rates are plotted in Fig. 2 for one year and half. Water production peaks after one day, at less than 2 m^3/day. Then, desaturation of the reservoir increases the gas permeability and gas production peaks few days after the water, at more than 400 m^3/day (standard conditions). The bell shape of the production curve is related to the size of the reservoir and the outer boundary conditions. With a small reservoir and an impermeable boundary, a plateau is not observed. Integrating the production, the cumulative production tends to 8330 m^3 which is the total volume of gas initially present in the reservoir given the Langmuir's parameters (Table 1).

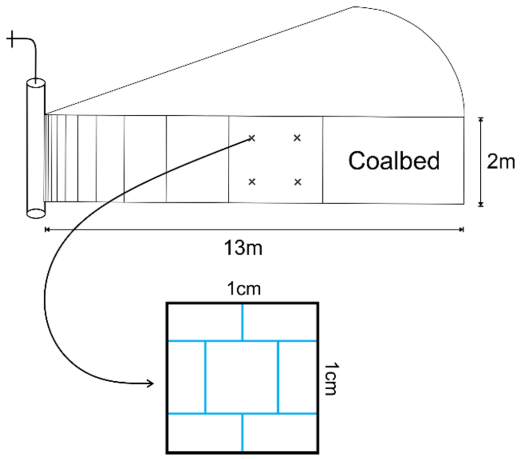

Fig. 1. Macroscale mesh and REV geometry.

Table 1. Parameters defining the reference case. *Aperture and stiffness given for a null stress.

Parameters	Values
Seam thickness (m)	2
Drainage radius (m)	13
Temperature (K)	293.15
Water pressure (Pa)	3E6
Gas pressure (Pa)	3E6
Overburden pressure (Pa)	5E6
Well transmissibility T (m^3)	1E-10
Coal density ρ_c (kg/m^3)	1500
Matrix Young's modulus E_m (Pa)	1.21E9
Matrix Poisson's ratio ν_m	0.16
Matrix width w (m)	0.005 – 0.01
Cleat aperture* h (m)	20E-6
Cleat normal stiffness* K_n (Pa/m)	100E9
Cleat shear stiffness K_s (Pa/m)	100E9
Minimum cleat aperture (m)	1E-6
Sorption time $\mathcal{T}$ (hours)	10
Langmuir volume V_L (m^3/kg)	0.02
Langmuir pressure P_L (Pa)	1.5E6
Matrix shrinkage coefficient β_ϵ (kg/m^3)	0.4
Entry capillary pressure p_e (Pa)	1E5
Distribution index λ	0.25
Residual water saturation $S_{r,res}$	0.1
Residual gas saturation	0.0

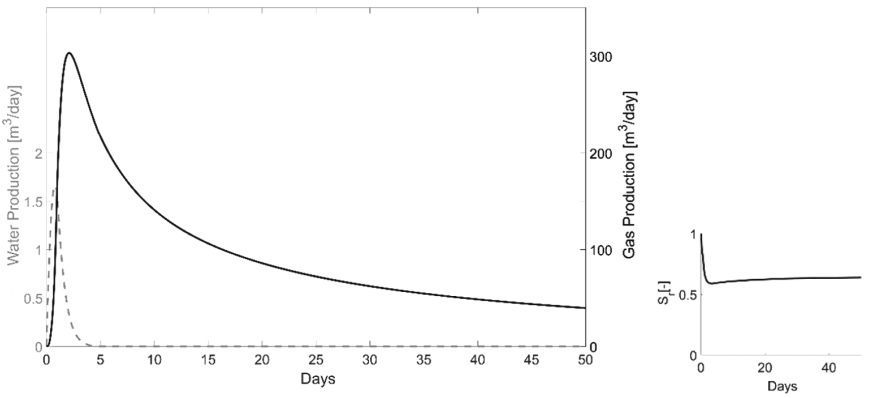

Fig. 2. Gas and water production curves with the corresponding evolution of the saturation degree.

4 Conclusions

The localization and homogenization procedure of the FE^2 method was used to extend our cleat-scale model (Bertrand et al. 2019) from the laboratory scale to the reservoir scale. The model was implemented in the Lagamine code and few contributions have been made in the purpose of coalbed methane production modelling (or reversely CO2 storage modelling). Mainly, a new degree of freedom for gas was introduced to deal with multiphase flow and a mechanism to account for swelling/shrinkage due to

sorption/desorption was implemented. This model was applied to the modelling of one production well.

Compared to macroscale models, any fracture network could be used in the REV geometry of the multiscale model. Indeed, macroscale models are limited to a matchstick geometry while, despite simple unit cells were used in our modelling, this is not a limitation of the multiscale model. Moreover, as physical phenomena are written at the fracture scale, the formulation can be simplified.

So, new sophisticated tools are now available to model multiphase flow in naturally fractured medium after the implementation of this extended FE^2 model. The model was applied to methane recovery but it could also be applied to carbon storage.

Acknowledgements. These researches were supported by the FNRS-FRIA and the WBI.

References

Bandis, S., Lumsden, A., Barton, N.: Fundamentals of rock joint deformation. Int. J. Rock Mech. Min. Sci. Geomech. Abs. **20**, 249–268 (1983)

Bertrand, F., Buzzi, O., Collin, F.: Cleat-scale modelling of the coal permeability evolution due to sorption-induced strain. Int. J. Coal Geol. **216**, 103320 (2019)

Bertrand, F., Cerfontaine, B., Collin, F.: A fully coupled hydro-mechanical model for the modeling of coalbed methane recovery. J. Nat. Gas Sci. Eng. **46**, 307–325 (2017)

Brooks, R.H., Corey, A.T.: Hydraulic properties of porous media and their relation to drainage design. Trans. ASAE **7**(1), 26–0028 (1964)

Goodman, R.E.: Methods of geological engineering in discontinuous rocks (1976)

Kouznetsova, V., Geers, M.G., Brekelmans, W.M.: Multi-scale constitutive modelling of heterogeneous materials with a gradient-enhanced computational homogenization scheme. Int. J. Numer. Methods Eng. **54**(8), 1235–1260 (2002)

Langmuir, I.: The adsorption of gases on plane surfaces of glass, mica and platinum. J. Am. Chem. Soc. **40**(9), 1361–1403 (1918)

Marinelli, F.: Comportement couplé des géo-matériaux: deux approches demodélisation numérique. PhD thesis, Université Grenoble Alpes (2013)

Özdemir, I., Brekelmans, W., Geers, M.: Computational homogenization for heat conduction in heterogeneous solids. International journal for numerical methods in engineering, 73(2):185–204 (2008)

Su, F., Larsson, F., Runesson, K.: Computational homogenization of coupled consolidation problems in micro-heterogeneous porous media. Int. J. Numer. Methods Eng. **88**(11), 1198–1218 (2011)

Van den Eijnden, B.: Multi-scale modelling of the hydro-mechanical behaviour of argillaceuous rocks. PhD thesis, Université Grenoble Alpes (2015)